JACS
JOURNAL OF THE AMERICAN CHEMICAL SOCIETY
Article
pubs.acs.org/JACS

^{19}F NMR Fingerprints: Identification of Neutral Organic Compounds in a Molecular Container

Yanchuan Zhao, Georgios Markopoulos, and Timothy M. Swager*

Department of Chemistry, Massachusetts Institute of Technology, Cambridge, Massachusetts 02139, United States

Supporting Information

ABSTRACT: Improved methods for quickly identifying neutral organic compounds and differentiation of analytes with similar chemical structures are widely needed. We report a new approach to effectively "fingerprint" neutral organic molecules by using ^{19}F NMR and molecular containers. The encapsulation of analytes induces characteristic up- or downfield shifts of ^{19}F resonances that can be used as multidimensional parameters to fingerprint each analyte. The strategy can be achieved either with an array of fluorinated receptors or by incorporating multiple nonequivalent fluorine atoms in a single receptor. Spatial proximity of the analyte to the ^{19}F is important to induce the most pronounced NMR shifts and is crucial in the differentiation of analytes with similar structures. This new scheme allows for the precise and simultaneous identification of multiple analytes in a complex mixture.

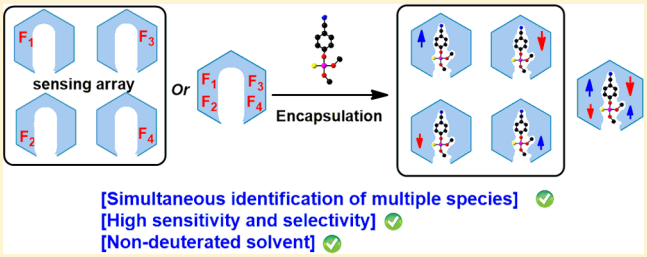

INTRODUCTION

There is an increasing awareness of the need for more selective and reliable methods to detect and rapidly identify target analytes of interest in a variety of contexts relevant to health care, process control, and environmental monitoring.[1] Chemosensory systems designed to assist in this process are molecular constructs that respond to a stimulus and give a measurable change in electronic, optical, and/or chemical/spectroscopic properties.[2] Transduction generally involves molecular associations or an electron transfer process between the analyte and a receptor.[3] These interactions typically occur at a specific bonding site, and sensing methods based on this strategy are best suited to detect classes of structurally related analytes, but often fail in the precise discrimination of related species. Array sensing has emerged as an approach that increases discriminatory power by combining signals collected by a large amount of individual sensors.[4] However, without highly orthogonal discrimination between analytes, this method often has difficulty in unambiguously identifying analytes at unknown concentrations. Herein, we report a sensing method based on ^{19}F NMR and the encapsulation of an analyte with molecular containers. The method provides a unique spectroscopic signature (fingerprint) that allows for an output and enables precise and simultaneous identification of multiple guest molecules in a complex mixture.[5]

^{19}F NMR has emerged as a versatile tool in biological and pharmaceutical studies as a result of the high sensitivity and scarcity of naturally occurring background signals.[6] Libraries of fluorinated compounds are used to identify potential ligands that bind to target proteins.[7] Fluorinated biological molecules have utility in the determination of enzyme activity.[8] In addition to reaction monitoring, such as the hydrolysis of a fluorine-containing substrate, various metal ions can be detected through reversible association with fluorinated chelates or crown ethers where characteristic shifts are generated for each metal ion.[9] As the induced ^{19}F NMR shifts are largely dependent on the through-bond disturbance of electron density at the fluorine atom upon association, charged species are typically selected as target analytes. In contrast, the detection and differentiation of neutral organic molecules with similar structures represents a significant challenge for most sensing methods.

To achieve our goal of unique identification of an analyte, our platform needs to meet the following criteria: (1) The molecular recognition event is sufficiently defined to provide a well-structured binding complex. (2) There are a number of independently varying ^{19}F NMR signals that shift to provide a robust multidimensional discrimination of an analyte. (3) The shift of the ^{19}F resonance should be induced by spatial proximity rather than through-bond electron density transmission so that the structure information on the whole molecule can be accessed by spatially arranged fluorine atoms.

Molecular containers, such as cavitands and capsules with different levels of preorganization, have found wide-ranging applications in molecular recognition.[10] By design, the encapsulation of an analyte induces a change of the environment inside the container, thereby creating easily discernible ^{19}F NMR shifts. The multidimensional output can be achieved either with an array of receptors bearing equivalent fluorine atoms at different positions relative to the analyte (Scheme 1a) or by employing a single receptor with multiple nonequivalent fluorine atoms (Scheme 1b). As a result of the scarcity of organic fluorine compounds in nature,[6,11] it is unlikely that there will be interfering

Received: May 6, 2014
Published: July 22, 2014

   dx.doi.org/10.1021/ja504110f | J. Am. Chem. Soc. 2014, 136, 10683−10690

Scheme 1. Schematic Illustration of ^{19}F NMR Spectroscopy Identification of Organic Molecules with Molecular Containers

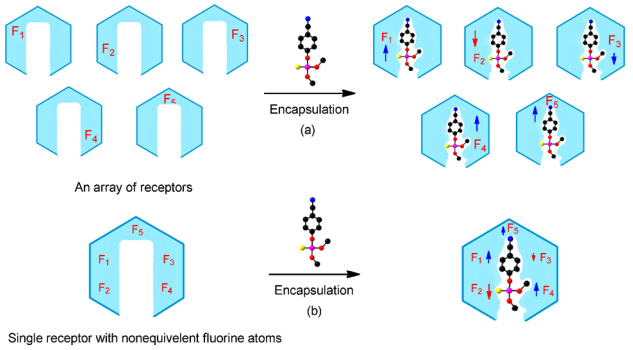

signals, and our scheme provides an efficient method to fingerprint a chosen analyte.[12]

RESULTS AND DISCUSSION

We chose calix[4]arene tungsten−imido complexes as a scaffold from which to produce partially fluorinated molecular containers on the basis of their synthetic accessibility and the fact that the Lewis acidic nature of the metal center gives predictable binding structures with Lewis basic analytes.[13] To evaluate the feasibility of the strategy based on encapsulation and the chemical shift induced by spatial proximity, we examined calixarene tungsten−imido complexes appended with spatially varying trifluoromethyl (CF_3) and trifluoromethoxy (OCF_3) groups at the upper rim (Scheme 2, complexes **1**−**4**). In addition to an array of complexes that can be employed together to output a fingerprint, receptors **5** and **5a** with multiple nonequivalent fluorine atoms are also prepared (Scheme 2).

Scheme 2. Fluorinated Calix[4]arene−Tungsten Complexes Employed in This Study

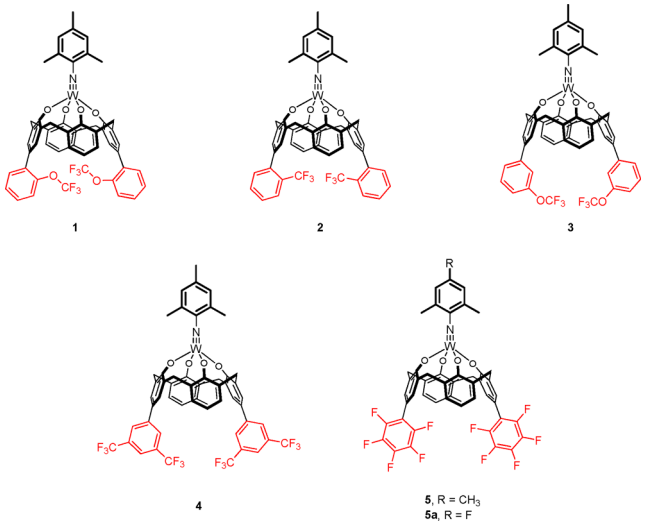

Synthesis. The $-CF_3$ and $-OCF_3$-substituted calix[4]arenes **7**−**10** were prepared through a Suzuki−Miyaura coupling of diiodocalix[4]arene (**6**) and various organoboronic acids followed by a demethylation with Me_3SiI (Scheme 3a). The target bis(pentafluorophenyl)-substituted calix[4]arene (**11**) was prepared through a silver-mediated direct coupling of **6**

Scheme 3. Preparation of Fluorinated Calix[4]arenes 7−11

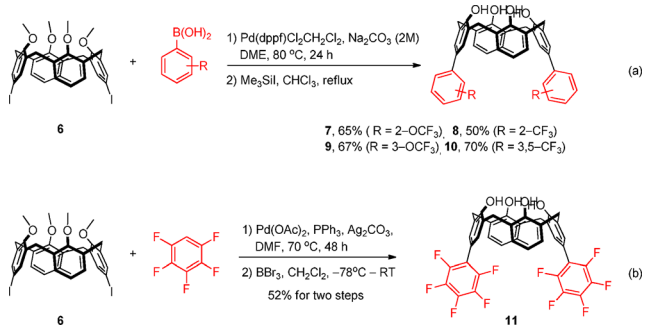

and pentafluorobenzene recently reported by Zhang and co-workers.[14] The methyl groups were subsequently removed by treatment with BBr_3 in CH_2Cl_2 at low temperature (Scheme 3b). The corresponding tungsten−imido complexes **1**−**5** were obtained using a previously reported "one-pot" procedure from calixarenes **7**−**11** by reaction with $WOCl_4$ and iminophosphorane ($Ph_3P{=}NR$) reagent.[15]

NMR Fingerprinting with an Array of Receptors. To evaluate the fidelity of this strategy in the precise identification of structurally similar molecules, we selected a series of nitriles with an interest in differentiating pesticides and pharmaceuticals.[16] The Lewis basic nitrile can be encapsulated in the molecular containers **1**−**5** and **5a** through the formation of a coordination bond with the tungsten atom. Sensing experiments are performed by adding analytes to chloroform solutions of **1** at ambient temperature. The formation of a static complex with **1** is critical to create a clear shift rather than a dynamic structure that will produce shifts that are more akin to a solvent effect.[15] In this way, the fluorine atoms provide discrete signals at precise shifts that are uniquely assignable to the encapsulated analytes. Notably, the $-OCF_3$ group in tungsten complex **1** appears as a singlet at −56.63 ppm (Figure 1a), which is very close to the shift found with parent calix[4]arene **7** (−56.51 ppm), indicating the remote through-bond effects are not efficient to induce a ^{19}F NMR shift. In contrast, the binding of nitriles to **1** produces 0.2−0.9 ppm downfield shifts in ^{19}F NMR as a result of the disturbance of the environment through replacement of solvent molecules by the analyte. Consistent with this model, acetonitrile induces a much smaller shift than less electron-donating 3-bromopropionitrile. All of our results are consistent with the differences in ^{19}F NMR of free and bound complex **1** being caused by spatial proximity rather than through-bond electron transmission (Figure 1d,g). The precision in the identification of molecules is illustrated by comparison of the differences induced by the binding of acetonitrile, propionitrile, and nonanenitrile with **1**. In this experiment, nonanenitrile induces a more pronounced downfield shift than propionitrile and acetonitrile (Figure 1d−f). The power of this method was further evaluated by the analysis of a mixture with a number of potential guest molecules. In this experiment, a mixture of nine different nitriles and **1** gave the same spectrum as obtained by superimposing the spectra recorded with each analyte independently (Figure 1b,c). It is notable that the precise identification of the multiple neutral organic analytes in a mixture represents a powerful advance in chemical sensing.

We next explored the sensing properties of 2-CF_3-substituted complex **2**. Interestingly, although the encapsulation of alkyl nitriles (Figure 2d−h) and benzyl nitriles (Figure 2i,j) produces downfield shifts which are also observed in the experiments with **1**,

dx.doi.org/10.1021/ja504110f | J. Am. Chem. Soc. 2014, 136, 10683−10690

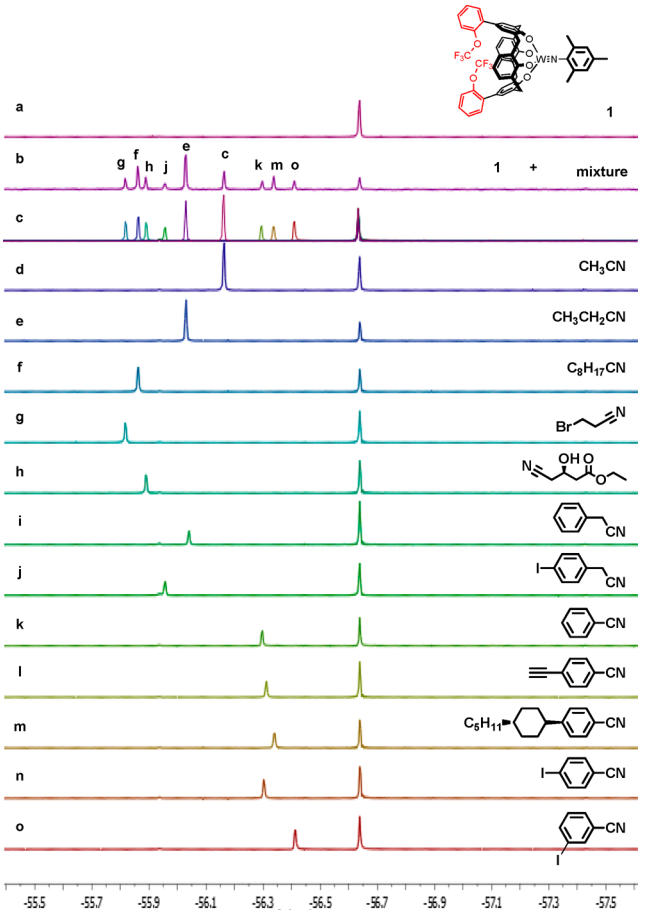

Figure 1. ^{19}F NMR spectra (64 scans) of complex **1** alone and mixtures of complex **1** (1.0 mM in $CDCl_3$) and different analytes (2.0 mM): (a) complex **1** alone, (b) nine nitriles added to a solution of **1** in $CDCl_3$, (c) superimposition of the spectra of complex **1** with each of the nine nitriles from (b) collected independently, (d)−(o) complex **1** bound to various nitriles.

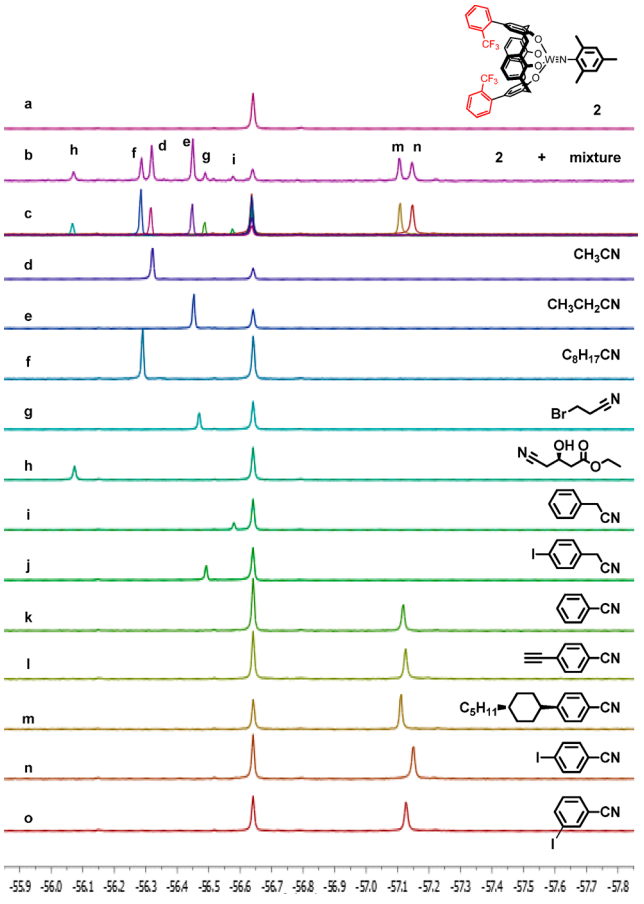

Figure 2. ^{19}F NMR spectra (64 scans) of complex **2** alone and mixtures of complex **2** (1.0 mM in $CDCl_3$) and different analytes (2.0 mM): (a) complex **2** alone, (b) eight nitriles added to a solution of **2** in $CDCl_3$, (c) superimposition of the spectra of complex **2** with each of the eight nitriles from (b) collected independently, (d)−(o) complex **2** bound to various nitriles.

aromatic nitriles (Figure 2k−o) induced upfield shifts upon binding, thus providing a facile way to determine the identity of the analyte. Unlike the trend observed in the experiments with **1**, the bonding of 3-bromopropionitrile with **2** gives a smaller downfield shift than that of acetonitrile and nonanenitrile (Figure 2d−g). This result indicates receptors/sensors with orthogonal discriminatory power can be easily produced by incorporating fluorine atoms at different positions. Similarly, complex **2** also shows the ability to identify a series of nitriles in a complex mixture (Figure 2b).

The differences observed for individual analytes are shown in Figures 1 and 2, and the characteristic up- and downfield shifts induced by each analyte are given in a two-dimensional plot, with the ^{19}F resonances of **1** and **2** as the axes (Figure 3). Simple inspection of these data reveals the ability of the combined sensor system to resolve all the alkyl and benzyl nitriles. In contrast, the discrimination of benzonitriles with the *para*-substituents investigated is still not satisfactory probably because the remote substituent only results in a minimal magnetic influence on the fluorine atoms in receptors **1** and **2**. Consistent with this assumption, 3-iodobenzonitrile with the substituent closer to the fluorine atom displays behavior different from that of *para*-substituented nitriles (Figure 3). It should be mentioned that a difference of 0.03 ppm leads to a baseline separation of singlet peaks in our ^{19}F NMR spectra, which correlates to a magnitude of 30 on the axes used in Figure 3.

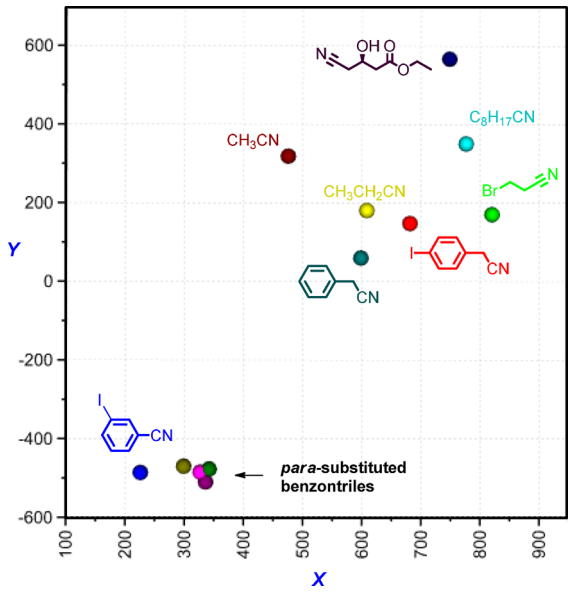

Figure 3. 2D scatter of analytes based on the shifts of ^{19}F resonances upon bonding: *x* axis, OCF_3 fluorine (**1**) ($-\Delta\delta \times 1000$); *y* axis, CF_3 fluorine (**2**) ($-\Delta\delta \times 1000$).

dx.doi.org/10.1021/ja504110f | J. Am. Chem. Soc. 2014, 136, 10683−10690

To achieve better resolution of benzonitriles, we examined complexes **3** and **4** with $-OCF_3$ and $-CF_3$ groups in the *meta*-position, respectively (Scheme 2). By design, the fluorine atoms in these complexes are closer to the *para*-substituent of the nitrile guests, which allows discrimination of this remote structural difference that was not achieved by **1** and **2**. As shown in Figures 4

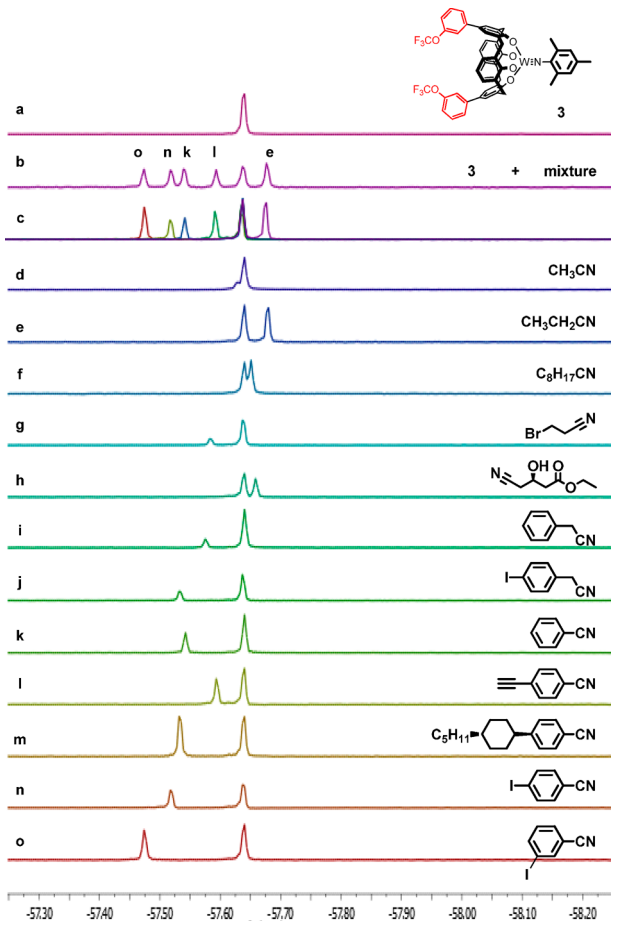

Figure 4. ^{19}F NMR spectra (64 scans) of complex **3** alone and mixtures of complex **3** (1.0 mM in $CDCl_3$) and different analytes (2.0 mM): (a) complex **3** alone, (b) four aromatic nitriles and propionitrile added to a solution of **3** in $CDCl_3$, (c) superimposition of the spectra of complex **3** with each of the five nitriles from (b) collected independently, (d)–(o) complex **3** bound to various nitriles.

and 5, the differences in ^{19}F NMR of free and bound complexes are within the range of <0.3 ppm, which is smaller than those observed with **1** and **2**, suggesting spatial proximity is crucial to induce shifts. Minimum ^{19}F NMR shifts are observed for acetonitrile as a result of its smaller size (Figures 4d and 5d). Interestingly, despite the smaller shifts produced, complexes **3** and **4** display improved resolution of benzonitriles relative to complexes **1** and **2** as shown in Figures 4k–o and 5k–o. Our collective results indicate it is possible to rationally design sensors with the desired selectivity by optimizing the position of the fluorine atoms. Simultaneous discrimination of diverse benzonitriles in a mixture is further demonstrated by the well-dispersed peaks shown in Figures 4b and 5b.

Multiple sensors with orthogonal discriminatory properties allow for higher analyte resolution through a combined analysis of signals from multiple receptors. Figure 6 is a plot using the ^{19}F NMR differences observed with **1** and **4**. As a result of the orthogonal selectivity imparted by the spatial distribution

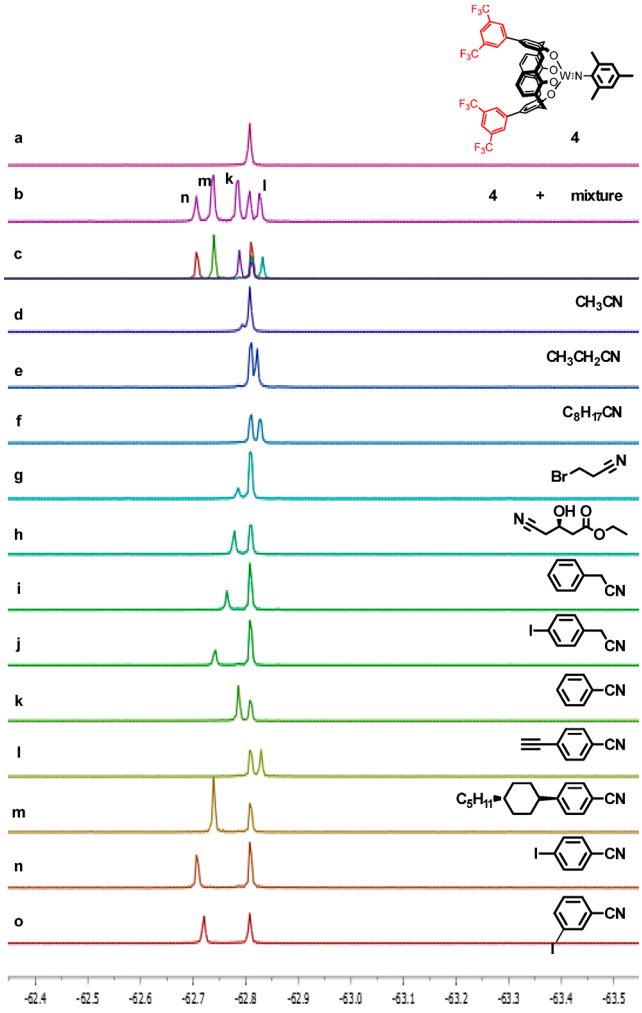

Figure 5. ^{19}F NMR spectra (64 scans) of complex **4** alone and mixtures of complex **4** (1.0 mM in $CDCl_3$) and different analytes (2.0 mM): (a) complex **4** alone, (b) four aromatic nitriles added to a solution of **4** in $CDCl_3$, (c) superimposition of the spectra of complex **4** with each of the four nitriles from (b) collected independently, (d)–(o) complex **4** bound to various nitriles.

variance, this combination provides better resolution than that shown in Figure 3 wherein **1** and **2** were employed. Moreover, the resolution can be further enhanced by using signals collected by a third receptor. The use of **1**, **2**, and **4** enables an interpretable 3D differentiation of all the analytes. As shown in Figure 7, all aromatic nitriles appear below the *xy* plane, benzyl nitriles give pronounced *x* values, and alkyl nitriles give smaller *x* values. Simple inspection of these figures reveals utility for the facile classification of analytes.

NMR Fingerprinting with a Single Receptor. The preceding studies enable the development of a receptor with multiple nonequivalent fluorine atoms that can fingerprint organic nitriles. In this regard, in addition to pentafluorophenyl groups, we have also incorporated a fluorine atom on the arylimido group, which has been shown to differentiate the electron-donating ability of the bound analytes by ^{19}F NMR shifts.[15] By design, the pentafluorophenyl group of **5a** spatially arranges fluorine groups in a polarizable π-system to create an environment capable of differentiating structurally similar analytes (Figure 1). The NMR experiments were carried out similarly to those of complexes **1**–**4**. As shown in Figure 8, the *imido*-fluorine of **5a** appears as a triplet at around −100 (t) ppm,

dx.doi.org/10.1021/ja504110f | J. Am. Chem. Soc. 2014, 136, 10683–10690

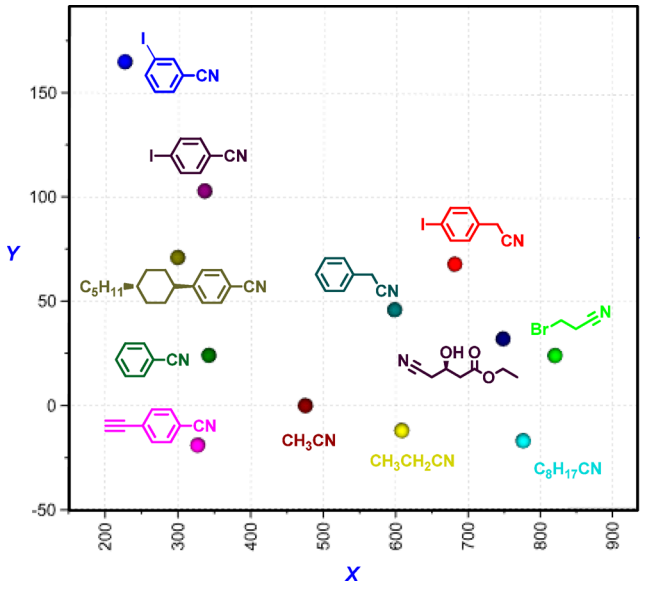

Figure 6. 2D scatter of analytes based on the shifts of ^{19}F resonances upon bonding: *x* axis, 2-$OCHF_3$ fluorine (**1**) ($-\Delta\delta \times 1000$); *y* axis, 3,5-$CF_3$ fluorine (**4**) ($-\Delta\delta \times 1000$).

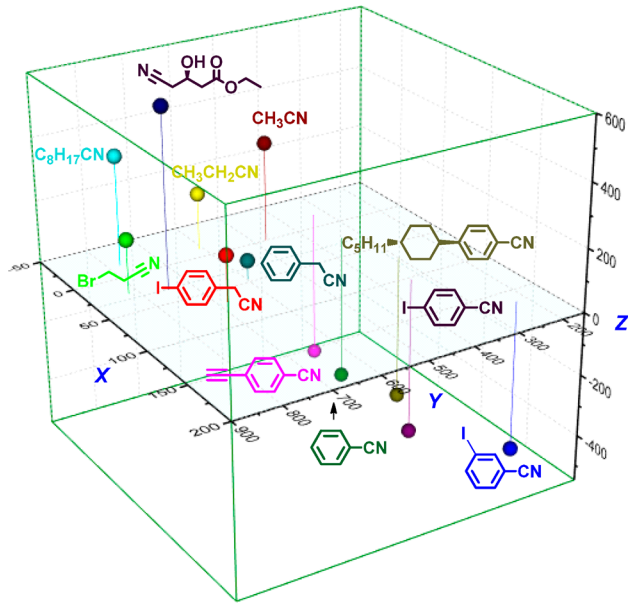

Figure 7. 3D scatter of analytes based on the shifts of ^{19}F resonances upon bonding: *x* axis, 3,5-CF_3 fluorine (**4**) ($-\Delta\delta \times 1000$); *y* axis, 2-$OCF_3$ fluorine (**1**) ($-\Delta\delta \times 1000$); *z* axis, 2-$CF_3$ fluorine (**2**) ($-\Delta\delta \times 1000$).

and the peaks at −143 (dd), −156 (t), and −162 (m) ppm are identified as *o*-, *p*-, and *m*-fluorine, respectively (Figure 8a). These distinctive chemical shifts provide a multidimensional spectroscopic signature without complexity from overlapping ^{19}F NMR signals. Binding of nitriles to **5a** produces upfield shifts in the ^{19}F NMR of the pentafluorophenyl group as a result of the shielding effects of the encapsulated molecules. Alkyl nitriles with varying chain length from acetonitrile to nonanenitrile display increasing upfield shifts for the *imido*-fluorine which correlate with the electron-donating ability of these molecules to the tungsten center (Figure 8d−g), and the same trend is observed for substituted aromatic nitriles (Figure 8k−n). Pronounced upfield shifts of *m*-^{19}F signals are observed with aromatic nitriles and provide a differentiation from the alkyl nitriles investigated (Figure 8k−o). In contrast, benzyl nitrile did not induce a shift of *m*-^{19}F signals, thereby indicating the importance of the precise position of the aromatic group in the molecular container (Figure 8i). It is also notable that 4-iodobenzonitrile induces less pronounced upfield shifts of *m*- and *p*-^{19}F NMR signals as compared to benzonitrile (part n vs part k of Figure 8), indicating a downfield shifting effect with halide substitution. This trend is also observed for 4-iodobenzyl cyanide and 3-bromopropionitrile, which induce downfield shifts of *m*- and *p*-^{19}F NMR signals. The downfield shifts relative to the shifts for the uncomplexed receptor are not surprising because only very small upfield shifts are produced by their nonhalogenated analogues (part j vs part i and part g vs part d of Figure 8). Electron-rich aromatic nitriles produce a more pronounced upfield shift of *m*- and *p*-^{19}F NMR signals as compared to electron-deficient aromatic nitriles, and this trend is also displayed by the shifts in the *imido*-^{19}F NMR signals, which are solely dependent upon the electron-donating ability of the nitriles (Figure 1k−n). Owing to the polarizable π-system, **5a** is more sensitive to the electronic properties of aromatic nitrile than **1**−**4**. As a result of the multiplets of the ^{19}F NMR, the overlap of signals produced by each analyte is more likely in the analysis of a complex mixture (Figure 8b).

The selective detection/identification of insecticides is important considering the widespread usage and toxicity of these chemicals. Cyanophos [*O*-(4-cyanophenyl) *O*,*O*-dimethyl phosphorothioate] is an organophosphorus-based insecticide that is effective against various plant pests.[17] It is a powerful cholinesterase inhibitor and represents a threat to human health. Traditional chemosensing methods typically rely on bonding or reactions with the Lewis acidic phosphorus group, which is not readily distinguished from structurally related compounds.[18] In contrast, our method generates a fingerprint that precisely distinguishes this compound from all other analytes (Figure 8p). Notably, the characteristic upshift of *m*-fluorine enables a fast assignment of cyanophos as an aromatic nitrile. This method was able to provide unambiguous detection of the cyanophos signals (S/N > 15) at an analyte concentration of 100 μM using a 400 MHz spectrometer and an acquisition time of 24 min (800 scans) (for details, see Figure S1 in the Supporting Information).

A three-dimensional plot is shown in Figure 9, with the *o*-, *p*-, and *m*-^{19}F NMR signals as the axes and the relative shift of the *imido*-^{19}F NMR signal represented by the radius of a sphere. The highly dispersed data points demonstrated the ability of **5a** to resolve all the analytes. As expected, nitriles with similar structures display ^{19}F NMR signals that are close to one another. For example, acetonitrile and propionitrile (Figure 8d,e) induce similar but differentiated responses. It should be mentioned that the radii of the spheres in Figure 9 correlate with the shift of *imido*-fluorine and can further differentiate analytes that produce similar spectral differences in the other ^{19}F NMR signals, such as ethyl (*R*)-4-cyano-3-hydroxybutyrate (Figure 8h) and $C_8H_{17}CN$ (Figure 8f).

Association Constants and Detection Limits. The association constants were measured in chloroform. The concentrations of free and bound complexes are determined by the integration of the ^{19}F NMR signal, and the concentration of free nitrile is calculated accordingly. As shown in Table 1, the magnitude of the bonding constant varies significantly toward different nitriles. For **1** and **2**, the constants decrease in the sequence acetonitrile, benzonitrile, and benzyl nitrile. Significant bonding enhancement of benzonitrile is observed with **4**, **5**, and **5a**, indicating the favorable π−π interactions between the phenyl

dx.doi.org/10.1021/ja504110f | J. Am. Chem. Soc. 2014, 136, 10683−10690

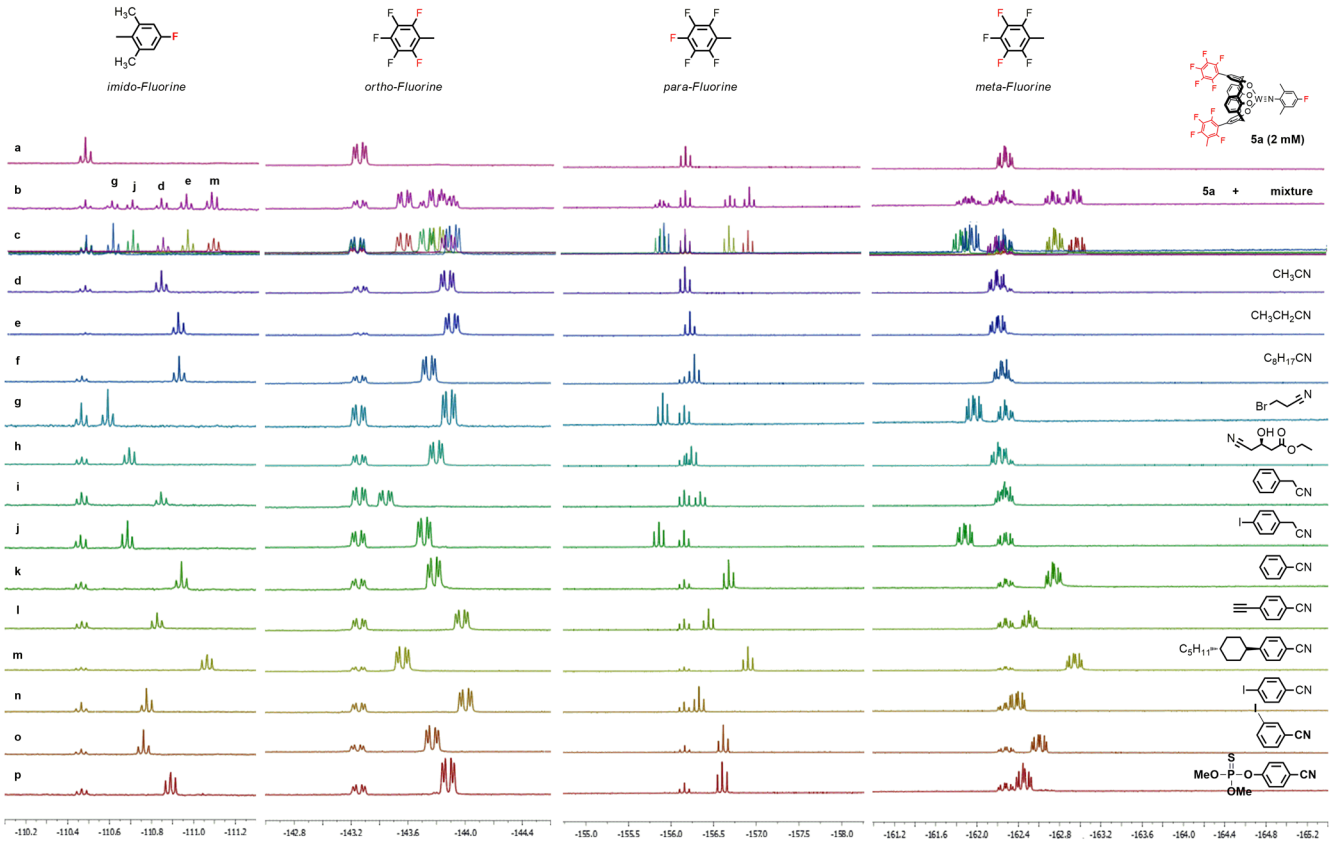

Figure 8. ^{19}F NMR spectrum (typically 128 scans) of a mixture of complex **5a** (2 mM in $CDCl_3$) and different analytes (5.0 mM). (a) Five nitriles were added to a solution of **5a** in $CDCl_3$. (b) Superimposition of the spectrum collected independently. ^{19}F NMR spectra (typically 128 scans) of complex **5a** alone and mixtures of complex **5a** (2.0 mM in $CDCl_3$) and different analytes (5.0 mM): (a) complex **5a** alone, (b) five nitriles added to a solution of **5a** in $CDCl_3$, (c) superimposition of the spectra of complex **5a** with each of the five nitriles from (b) collected independently, (d)−(p) complex **5a** bound to various nitriles.

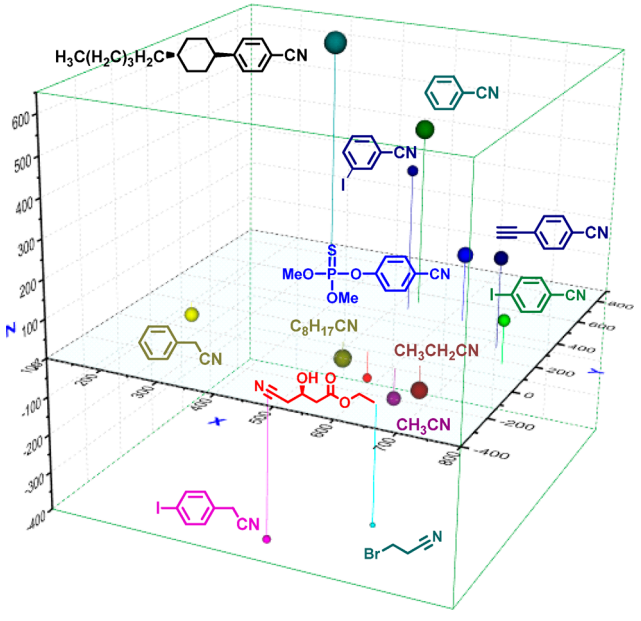

Figure 9. 3D scatter of analytes based on the shifts of ^{19}F resonances upon bonding: *x* axis, *o*-^{19}F ($-\Delta\delta \times 1000$); *y* axis, *p*-^{19}F ($-\Delta\delta \times 1000$); *z* axis, *m*-^{19}F ($-\Delta\delta \times 1000$). The sphere radius is correlated to *imido*-^{19}F ($-\Delta\delta \times 1000$) with a factor of 0.04.

ring and electron-deficient 3,5-bis(trifluoromethyl)phenyl or pentafluorophenyl group. Changing the methyl group to fluorine on the arylimido group is beneficial to the binding as a result of the increased Lewis acidity of the tungsten center. It should be mentioned that the dissociation of the internal bound ligand of a metalated cavitand tends to be slow because of the isolation of the ligand from the bulk solution. This explains why a relatively low binding constant is accompanied by a slow exchange system.[19] Notably, with the association constants, the simultaneous and quantitative measurements of multiple analytes can be achieved on the basis of signal integrations (for details, see Figure S8 in the Supporting Information). According to eq 1, the

Table 1. Association Constants (K/M^{-1}) of Various Nitriles with a Tungsten−Imido Complex[a]

	1	2	3	4	5	5a
K (CH_3CN)	945	815	*b*	*b*	618	786
K (PhCN)	345	372	279	897	852	1360
K ($PhCH_2CN$)	177	97	118	219	318	600

[a]Determined by ^{19}F NMR in $CDCl_3$. Three measurements at different concentrations are taken, and the average is given in the table, error <15%. [b]Not determined because the signals overlap in both ^{1}H NMR and ^{19}F NMR.

$$\text{CalixW(NR)} + \text{analyte} \overset{K}{\rightleftharpoons} \text{CalixW(NR)}\text{:(analyte)}$$

$$K = \frac{[\text{CalixW(NR)}\text{:(analyte)}]}{[\text{CalixW(NR)}][\text{analyte}]} \quad (1)$$

dx.doi.org/10.1021/ja504110f | J. Am. Chem. Soc. 2014, 136, 10683−10690

ratio of bound to free analyte is equal to K[CalixW(NR)]. For the detection of analyte in the presence of excess receptor, [CalixW(NR)] is the total complex concentration employed in the analysis. This means, for example, about 45% of the analyte is in the complexed form when a trace amount of benzonitrile is detected in the presence of 2 M tungsten complex **1**. Owing to the six equivalent fluorine atoms and singlet peak, the detection limit of benzonitrile in the presence of 2 M **1** is determined to be down to 10 μM using a 400 MHz spectrometer and an acquisition time of 24 min (800 scans) in contrast to the 100 μM detection limit of cyanophos obtained with **5a** (for details, see Figure S7 in the Supporting Information).

The robust sensing power is further demonstrated by the analysis of a complex mixture of various nitriles in the presence of an excess amount of hexane, ethyl acetate, and acetone with **1**. As shown in Figure 10, noncoordinating analytes, such as hexane,

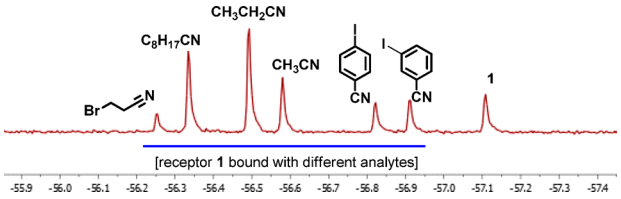

Figure 10. ^{19}F NMR spectrum (64 scans) of a mixture of complex **1** (ca. 0.8 mM in CH_2Cl_2), various nitriles (each ca. 1.6 mM), hexane (5 μL), ethyl acetate (5 μL), and acetone (5 μL).

ethyl acetate, and acetone, did not give signals, while various nitriles can be unambiguously identified simultaneously even in nondeuterated solvent.

The detection of pollution in water is crucial to environmental monitoring. Although many sensing methods are capable of detecting a specific target in domestic water, the analysis of a more complex matrix, such as river water, is still challenging. To mimic a sample in the environment, water taken from the Charles River between Boston and Cambridge, MA, was contaminated with cyanophos at various concentrations. To use a minimum amount of organic solvent, river water (5 mL) was extracted with a solution of receptor **1** in dichloromethane (2 M, 0.6 mL), and the resulting dichloromethane phase was analyzed by ^{19}F NMR. The detection limit of cyanophos is determined to be 5 μM by using this method (for details, see Figure S10 in the Supporting Information). Enrichment by extraction is often employed when detecting nanomolar range neutral organic molecules in water. As the process is not selective, a complex mixture with a number of components at much higher concentrations than the target analyte is often obtained. To test our method in the analysis of a mixture obtained from enrichment, river water (500 mL) was extracted with dichloromethane (100 mL × 3) and concentrated. The extract was then redissolved in a solution of receptor **1** in dichloromethane (2 M, 0.5 mL) and analyzed by ^{19}F NMR. Detection of cyanophos at 20 nM in river water was achieved by this method (for details, see Figure S11 in the Supporting Information). It is worth noting that a number of unidentified species at much higher concentrations than that of cyanophos were observed in ^{1}H NMR, which makes the identification of cyanophos unsuccessful in ^{1}H NMR (for details, see Figure S12 in the Supporting Information). The preceding studies are intended to illustrate that the method is sufficiently robust for demanding applications. A more efficient extraction process could be achieved by immobilization of **1** or analogues in a concentrator/filter assembly.

To gain more insight into the transduction of the current method, the X-ray single-crystal structures of **1**, **2**, and **5a** were obtained. Interestingly, **2**:CH_3CN is found to be perfectly isostructural to **1**:CH_3CN, and the only difference is the OCF_3 group is replaced by a CF_3 group (Figure 11). This result

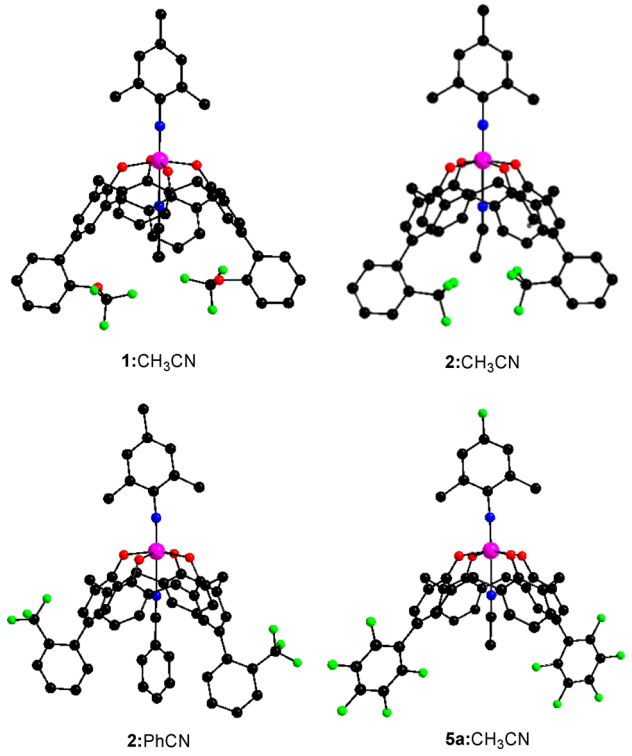

Figure 11. X-ray structures of **1**, **2**, and **5a** (1:1 cocrystal with CH_3CN or PhCN): black, carbon; green, fluorine; blue, nitrogen; red, oxygen; purple, tungsten. Note: The methyl groups of the acetonitriles in **1**:CH_3CN and **2**:CH_3CN are disordered about the crystallographic 2-fold axis.

suggests that it is valid to estimate the structures of related complexes. Although the nonlinear geometry of acetonitrile in **2**:CH_3CN is unusual, it is not unprecedented and has been observed in a variety of metal complexes.[20] Another observation is that fluorinated groups face inward for the cavity in **2**:CH_3CN whereas the opposite is true for **2**:PhCN. Probably as a result of the larger size of benzonitrile, the cavity of calixarene expands to fit the analyte. The discrete behaviors found in **2**:CH_3CN and **2**:PhCN in the crystal structure also shed light on the chemical shift induced with **2** wherein alkyl nitrile produces a downfield shift whereas aromatic nitrile induces an upfield shift (Figure 2). The distance of tungsten to the nitrogen of the nitrile in **2**:PhCN is significantly longer than that of **2**:CH_3CN (2.310 Å vs 2.287 Å), suggesting a weaker bonding of PhCN. This observation is consistent with the trend of association constants found in Table 1. It should be mentioned that the NMR signals are collected in solution; therefore, the shifts are largely dependent on the average distance between the fluorine atom and the analyte in all of the conformational isomers.

CONCLUSIONS

In summary, we have demonstrated a new sensing scheme based on ^{19}F NMR and the encapsulation of analytes with molecular containers. The method collects extensive interactions between the analyte and receptor/container to provide measurable signals

dx.doi.org/10.1021/ja504110f | J. Am. Chem. Soc. 2014, 136, 10683−10690

with sufficient dimensionality (information) to uniquely identify or "fingerprint" analytes that have only small structural differences. The strategy can be achieved either with an array of receptors or by incorporating multiple nonequivalent fluorine atoms in a single receptor. This new scheme allows for an informative and interpretable output and enables a precise and simultaneous identification of multiple potential guest molecules in a complex mixture. The structures we report herein are only representative examples and can be extended to many other structural scaffolds, including those targeting complex and/or larger biomolecular species that cannot be readily identified by conventional analytical methods (e.g., mass spectrometry). Critical to this latter prospect is the development of receptors/probes that incorporate ^{19}F groups that are sensitive to their environment and produce relatively static complexes. We envision these more complex recognition elements will produce powerful detection schemes relevant to environmental and biomedical sensing.

■ ASSOCIATED CONTENT

Supporting Information

Crystallographic data in CIF format, synthetic procedures and characterization of the compounds, NMR spectra, association constants, and detection limit studies. This material is available free of charge via the Internet at http://pubs.acs.org.

■ AUTHOR INFORMATION

Corresponding Author

tswager@mit.edu

Notes

The authors declare the following competing financial interest(s): A patent has been filed on the use of this method.

■ ACKNOWLEDGMENTS

This work was supported by a National Institutes of Health (National Institute of General Medical Sciences, NIGMS) grant (GM095843). Y.Z. acknowledges the Shanghai Institute of Organic Chemistry (SIOC), Zhejiang Medicine, and Pharmaron for a joint postdoctoral fellowship. G.M. thanks the German Academic Exchange Service (DAAD, postdoctoral fellowship). We thank Dr. Peter Müller for collecting and solving the X-ray structure data.

■ REFERENCES

(1) (a) Ho, C. K.; Robinson, A.; Miller, D. R.; Davis, M. J. *Sensors* **2005**, *5*, 4. (b) Krantz-Rulcker, C.; Stenberg, M.; Winquist, F.; Lundstrom, I. *Anal. Chim. Acta* **2001**, *426*, 217. (c) Du, J.; Hu, M.; Fan, J.; Peng, X. *Chem. Soc. Rev.* **2012**, *41*, 4511. (d) Pejcic, B.; Eadington, P.; Ross, A. *Environ. Sci. Technol.* **2007**, *41*, 6333. (e) Jun, Y.-W.; Lee, J.-H.; Cheon, J. *Angew. Chem., Int. Ed.* **2008**, *47*, 5122. (f) Kobayashi, H.; Ogawa, M.; Alford, R.; Choyke, P. L.; Urano, Y. *Chem. Rev.* **2010**, *110*, 2620. (g) Domaille, D. W.; Que, E. L.; Chang, C. J. *Nat. Chem. Biol.* **2008**, *4*, 168. (h) Lavis, L. D.; Raines, R. T. *ACS Chem. Biol.* **2008**, *3*, 142.

(2) (a) Czarnik, A. W. *Fluorescent Chemosensor for Ion and Molecule Recognition*; ACS Symposium Series 538; American Chemical Society: Washington, DC, 1993. (b) de Silva, A. P.; Gunaratne, H. Q. N.; Gunnlaugsson, T.; Huxley, A. J. M.; McCoy, C. P.; Rademacher, J. T.; Rice, T. E. *Chem. Rev.* **1997**, *97*, 1515. (c) Thomas, S. W., III; Joly, G. D.; Swager, T. M. *Chem. Rev.* **2007**, *107*, 1339. (d) Leray, I.; Valeur, B. *Eur. J. Inorg. Chem.* **2009**, *2009*, 3525. (e) Lange, U.; Mirsky, V. M. *Anal. Chim. Acta* **2011**, *687*, 105.

(3) Binghe, W.; Eric, V. A. *Chemsosensor: Principles, Strategies, and Applications*; John Wiley & Sons: Hoboken, NJ, 2011.

(4) (a) Diehl, K. L.; Anslyn, E. V. *Chem. Soc. Rev.* **2013**, *42*, 8596. (b) Askim, J. R.; Mahmoudi, M.; Suslick, K. S. *Chem. Soc. Rev.* **2013**, *42*, 8649. (c) Miranda, O. R.; Creran, B.; Rotello, V. M. *Curr. Opin. Chem. Biol.* **2010**, *14*, 728. (d) Wang, F.; Swager, T. M. *J. Am. Chem. Soc.* **2011**, *133*, 11181.

(5) For selected examples of NMR sensing to identify organic molecules, see: (a) Perrone, B.; Springhetti, S.; Ramadori, F.; Rastrelli, F.; Mancin, F. *J. Am. Chem. Soc.* **2013**, *135*, 11768. (b) Teichert, J. F.; Mazunin, D.; Bode, J. W. *J. Am. Chem. Soc.* **2013**, *135*, 11314.

(6) For a review discussing applications of ^{19}F NMR, see: Yu, J.-X.; Hallac, R. R.; Chiguru, S.; Mason, R. P. *Prog. Nucl. Magn. Reson. Spectrosc.* **2013**, *70*, 25.

(7) (a) Tengel, T.; Fex, T.; Emtenas, H.; Almqvist, F.; Sethson, I.; Kihlberg, J. *Org. Biomol. Chem.* **2004**, *2*, 725. (b) Dalvit, C.; Vulpetti, A. *Magn. Reson. Chem.* **2012**, *50*, 592.

(8) (a) Tanaka, K.; Kitamura, N.; Naka, K.; Chujo, Y. *Chem. Commun.* **2008**, 6176. (b) Tanaka, K.; Kitamura, N.; Chujo, Y. *Bioconjugate Chem.* **2011**, *22*, 1484. (d) Stockman, B. J. *J. Am. Chem. Soc.* **2008**, *130*, 5870. (e) Albert, M.; Repetschnigg, W.; Ortner, J.; Gomes, J.; Paul, B. J.; Illaszewicz, C.; Weber, H.; Steiner, W.; Dax, K. *Carbohydr. Res.* **2000**, *327*, 395. (f) Mendz, G. L.; Lim, T. N.; Hazell, S. L. *Arch. Biochem. Biophys.* **1993**, *305*, 252. (g) Yu, J.; Liu, L.; Kodibagkar, V. D.; Cui, W.; Mason, R. P. *Bioorg. Med. Chem.* **2006**, *14*, 326. (h) Yu, J.; Mason, R. P. *J. Med. Chem.* **2006**, *49*, 1991. (i) Yu, J.-X.; Kodibagkar, V. D.; Liu, L.; Mason, R. P. *NMR Biomed.* **2008**, *21*, 704.

(9) (a) Smith, G. A.; Hesketh, R. T.; Metcalfe, J. C.; Feeney, J.; Morris, P. G. *Proc. Natl. Acad. Sci. U.S.A.* **1983**, *80*, 7178. (b) Schanne, F. A. X.; Dowd, T. L.; Gupta, R. K.; Rosen, J. F. *Proc. Natl. Acad. Sci. U.S.A.* **1989**, *86*, 5133. (c) Levy, L. A.; Murphy, E.; Raju, B.; London, R. E. *Biochemistry* **1988**, *27*, 4041. (d) Smith, G. A.; Kirschenlohr, H. L.; Metcalfe, J. C.; Clarke, S. D. *J. Chem. Soc., Perkin Trans. 2* **1993**, 1205. (e) Jiang, Z.-X.; Feng, Y.; Yu, Y. B. *Chem. Commun.* **2011**, *47*, 7233.

(10) (a) Rudkevich, D. M.; Rebek, J. J. *Eur. J. Org. Chem.* **1999**, *1999*, 1991. (b) Asfari, Z.; Böhmer, V.; Harrowfield, J. M.; Vicens, J. *Calixarenes 2001*; Kluwer Academic Publishers: Dordrecht, The Netherlands, 2001. (c) Rudkevich, D. M. *Chem.—Eur. J.* **2000**, *6*, 2679. (d) Cram, D. J. *Science* **1983**, *219*, 1177.

(11) (a) Furuya, T.; Kamlet, A. S.; Ritter, T. *Nature* **2011**, *473*, 470. (b) Harper, D. B.; O'Hagan, D. *Nat. Prod. Rep.* **1994**, *11*, 123.

(12) A topology-based fluorine fingerprint descriptor has been used to predict the ^{19}F NMR chemical shift: Vulpetti, A.; Landrum, G.; Rüdisser, S.; Erbel, P.; Dalvit, C. *J. Fluorine Chem.* **2010**, *131*, 570.

(13) (a) Gramage-Doria, R.; Armspach, D.; Matt, D. *Coord. Chem. Rev.* **2013**, *257*, 776. (b) Kotzen, N.; Vigalok, A. *Supramol. Chem.* **2008**, *20*, 129. (c) Radius, U.; Attner, J. *Eur. J. Inorg. Chem.* **1999**, 2221. (d) Guillemot, G.; Solari, E.; Floriani, C.; Rizzoli, C. *Organometallics* **2001**, *20*, 607.

(14) Chen, F.; Min, Q.-Q.; Zhang, X. *J. Org. Chem.* **2012**, *77*, 2992.

(15) Zhao, Y.; Swager, T. M. *J. Am. Chem. Soc.* **2013**, *135*, 18770.

(16) (a) Fleming, F. F. *Nat. Prod. Rep.* **1999**, *16*, 597. (b) Fleming, F. F.; Yao, L.; Ravikumar, P. C.; Funk, L.; Shook, B. C. *J. Med. Chem.* **2010**, *53*, 7902.

(17) (a) Tomlin, C. D. S. *The Pesticide Manual: A World Compendium*; The British Crop Protection Council: Farnham, England, 1997; pp 282–283. (b) Romeh, A. A. *J. Environ. Health Sci. Eng.* **2014**, *12*, 38.

(18) (a) Obare, S. O.; De, C.; Guo, W.; Haywood, T. L.; Samuels, T. A.; Adams, C. P.; Masika, N. O.; Murray, D. H.; Anderson, G. A.; Campbell, K.; Fletcher, K. *Sensors* **2010**, *10*, 7018. (b) Aragay, G.; Pino, F.; Merkoçi, A. *Chem. Rev.* **2012**, *112*, 5317.

(19) Le Poul, N.; Douziech, B.; Zeitouny, J.; Thiabaud, G.; Colas, H.; Conan, F.; Cosquer, N.; Jabin, I.; Lagrost, C.; Hapiot, P.; Reinaud, O.; Le Mest, Y. *J. Am. Chem. Soc.* **2009**, *131*, 17800.

(20) (a) Feng, S. G.; Gamble, A. S.; Philipp, C. C.; White, P. S.; Templeton, J. L. *Organometallics* **1991**, *10*, 3504. (b) Hutchinson, D. J.; Cameron, S. A.; Hanton, L. R.; Moratti, S. C. *Inorg. Chem.* **2012**, *51*, 5070. (c) Li, C.-P.; Chen, J.; Du, M. *CrystEngComm* **2010**, *12*, 4392. (d) Fox, S.; Stibrany, R. T.; Potenza, J. A.; Knapp, S.; Schugar, H. J. *Inorg. Chem.* **2000**, *39*, 4950. (e) Fernandez, E. J.; Laguna, A.; Lopez-de-Luzuriaga, J. M.; Monge, M.; Montiel, M.; Olmos, M. E.; Rodriguez-Castillo, M. *Dalton Trans.* **2009**, 7509.